Further Visualization of Combined Wing Tip and Starting Vortex Systems

P. Freymuth,* F. Finaish,† and W. Bank‡
University of Colorado, Boulder, Colorado

The combined wing tip and starting vortex systems of a variety of wing planforms have been visualized in a starting flow of constant acceleration. Movie sequences display the initial development of a variety of interesting vortex systems generated by these flow configurations. Vortices always formed closed systems in accordance with Helmholtz's law.

Introduction

THE concept of a combined vortex system consisting of a bound vortex, the tip vortices, and the starting vortex for wings of finite span was introduced by Prandtl[1,2] 70 years ago. Parts of this concept were introduced even earlier, i.e., the bound vortex by Kutta[3] (see also the historical remarks by Tani[4]) and the tip vortices by Lanchester[5] (see also the historical remarks by von Kármán[6] and Rogers[7]). Despite the long history of this topic of unsteady, incompressible and partly inviscid fluid dynamics, the overall vortex system and its development is visualized only recently, since appropriate visualization methods have been lagging. The state-of-the-art of flow visualization for finite wings in unsteady flow, which includes high angles of attack, has been reviewed in detail by Gad-el-Hak and Ho.[8] At high angles of attack, the bound vortex on the suction side of a wing can become a leading-edge free vortex as a result of boundary-layer separation, which adds to the complexity of the overall vortex system. According to Gad-el-Hak and Ho,[8] visualizations of unsteady, three-dimensional wing flows have focused on the two-dimensional cuts of dye-layer visualization in water[8,9] and on the cuts achieved by the smoke-wire technique in air.[10] As has been recognized,[8] it is very hard to reconstruct the overall vortex structure from such cuts. Similar problems are posed by the method of dye injection through holes in the wing as applied by Werlé[11,12] in water.

A way out of this dilemma is the use of a vortical tagging technique in air, whereby smoke is introduced as uniformly as possible on the vorticity-producing wing surfaces. The smoke then tags the vorticity and makes the overall vortex system visible. Liquid titanium tetrachloride ($TiCl_4$), which has been previously used by the authors[13] for two-dimensional visualizations, serves as a smoke-generating agent. This new concept of three-dimensional visualization in unsteady flow has been successfully introduced by Freymuth and his co-workers,[14-16] mainly to visualize the starting flow around half-wings. This method has its own limitations, since the smoke cannot be introduced quite homogeneously. However, the progress made toward global visualization of three-dimensional vortex systems is still remarkable. For the first time, an overall view of unsteady three-dimensional vortex development over a lifting surface has become available.

Received Sept. 8, 1986; revision received Jan. 27, 1987.

*Professor, Department of Aerospace Engineering Sciences.
†Graduate Student, Department of Aerospace Engineering Sciences. Member AIAA.
‡Electronic Engineer, Department of Aerospace Engineering Sciences.

The purpose of this paper is to extend this new visualization method to a variety of finite wing planforms in order to add experience and depth to this approach and to the understanding of wing vortex systems in highly complex situations. Visualizations of this kind should stimulate interest in corresponding computer simulations and serve as a verification source for numerical solutions. For two-dimensional unsteady flows over airfoils, computer solutions are already forthcoming.[17-19]

While we restrict ourselves to starting flows of constant acceleration, we anticipate that similar progress can be made in the visualization of impulsive starting flow over wings and of steady flow over pitching wings.

There exists a technological drive for the investigation of three-dimensional unsteady vortical flow over wings at high angle of attack. It is anticipated that such flows are important for fast-maneuvering, high-performance aircraft as has been explained in detail by Gad-el-Hak and Ho.[8]

It has been stated programmatically by McCroskey[20] that the main thrusts of unsteady fluid dynamics need to be directed to three-dimensional effects. Our present investigation should be considered in the light of this statement.

Experimental Methods

A wing of finite aspect ratio is held by means of two thin wires in the test section of a wind tunnel with cross section of 0.9×0.9 m. The tunnel is of the open-return type with a settling chamber upstream of the test section and with the fan located downstream, as sketched in Fig. 1. This arrangement yielded a swirl-free flow with a low turbulence level of order 0.1% in the test section. The flow in the tunnel starts from rest and sustains an almost constant acceleration $a = 2.4$ m/s^2 for 5 s. Thereafter, the electrical power to the fan motor is shut off and the tunnel is allowed to come to rest. The tunnel is ready for the next acceleration run within 2 min. The 186 kW electric dc motor that drives the fan is powered from a motor-generator set with field control at the generator. The current for field control does not exceed 2 A. For proper flow acceleration after start from rest, a current pulse was introduced into the field coil followed by a current ramp. Pulse duration and ramp slope were empirically adjusted for optimum performance.

The wings were made from flat aluminum sheets of 1.6 mm thickness that allowed easy manufacture of different planforms. The wings were adjusted to an angle of attack $\alpha = 40$ deg. The suction side of the wing could be observed through the Plexiglas sidewall of the tunnel. Smoke-generating liquid titanium tetrachloride ($TiCl_4$) was introduced prior to flow startup by means of a small brass pipette near all edges of the wing where vorticity generation was expected to occur, such that smoke release becomes indicative of vortical structures. The wing and white smoke were

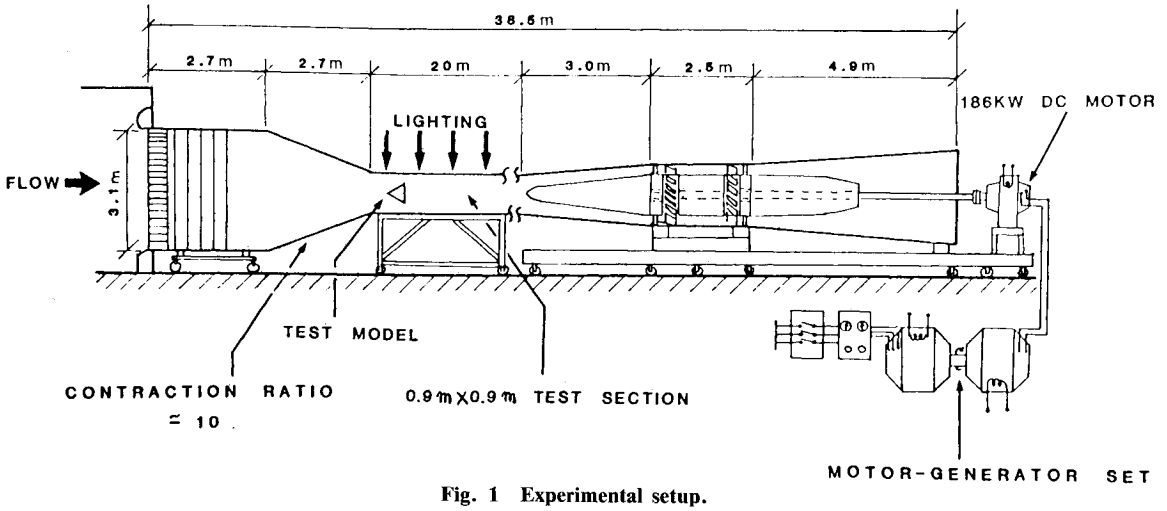

Fig. 1 Experimental setup.

GEOMETRY	SKETCH	GEOMETRIC PARAMETERS	VISUALIZATIONS APPEAR IN FIGURE
RECTANGULAR WING (SQUARE)	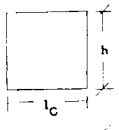	h = 15.2 cm l_c = 15.2 cm	(3)
RECTANGULAR WING	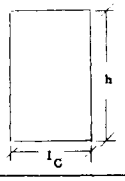	h = 30.4 cm l_c = 15.2 cm	(4)
DELTA WING	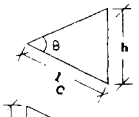	h = 15.2 cm l_c = 15.2 cm θ = 60°	(5)
DELTA WING IN REVERSE	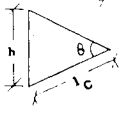		(6)
SAIL WING	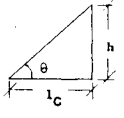	h = 15.2 cm l_c = 15.2 cm θ = 45°	(7)
SAIL WING IN REVERSE	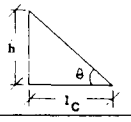		(8)
CIRCULAR WING	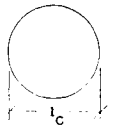	l_c = 15.2 cm d = 5.8 cm	(9)
CIRCULAR WING WITH CENTER HOLE			(10)

Fig. 2 Description of wing planforms and dimensions (note that these shapes will be given a 40 deg angle of attack when mounted in the wind tunnel and that $R = 5200$, $\Delta t^* = 0.25$, $t_1^* = 0.75$).

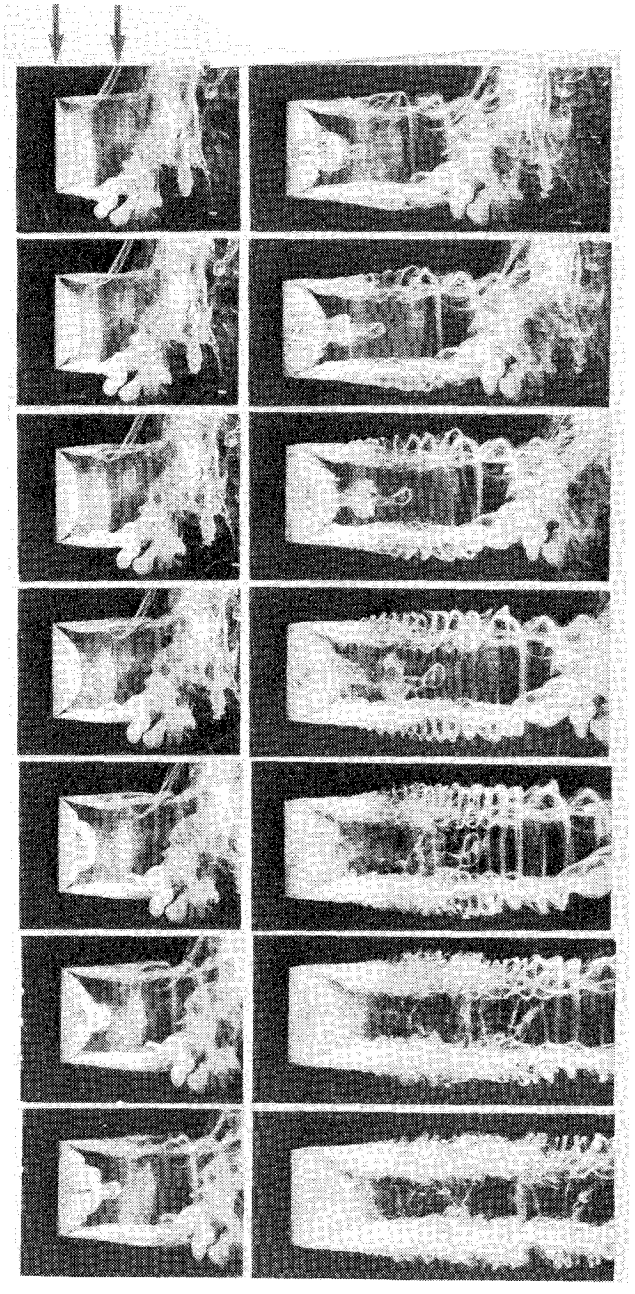

Fig. 3 Visualization sequence for rectangular (square) wing.

floodlit from the top and observed through the Plexiglas sidewall of the test section by using a Bolex movie camera with a rate of 64 frames/s. The frames have been assembled into figures showing the generation and development of vortical structures.

Dimensional Considerations

Before representing experimental results, it seems useful to enumerate the important scales and the dimensionless flow parameters of accelerated starting flow. We follow closely the account given by Freymuth[13] for two-dimensional accelerated starting flow over airfoils.

By means of the flow acceleration a and the wing characteristic length l_c as indicated in Fig. 2, a characteristic time t_c can be defined as

$$t_c = l_c^{1/2} a^{-1/2} \tag{1}$$

and a characteristic velocity V_c as

$$V_c = l_c^{1/2} a^{1/2} \tag{2}$$

From the classical definition of Reynolds number $R = V_c l_c/\nu$, then R can be written as

$$R = a^{1/2} l_c^{3/2}/\nu \tag{3}$$

where $\nu = 0.176$ cm^2/s is the air kinematic viscosity. Additional dimensionless parameters used to characterize the flow are the dimensionless time

$$t^* = t/t_c \tag{4}$$

(where t is the time counted from flow startup) and geometric parameters such as the angle of attack α and the various wing planforms.

The emphasis in this paper is on the influence of the various planforms. The angle of attack has been kept constant at $\alpha = 40$ deg for all wings. Furthermore, for all wings, the characteristic length was kept at $l_c = 15.2$ cm and the acceleration after start was $a = 2.4$ m/s^2. Then, the character-

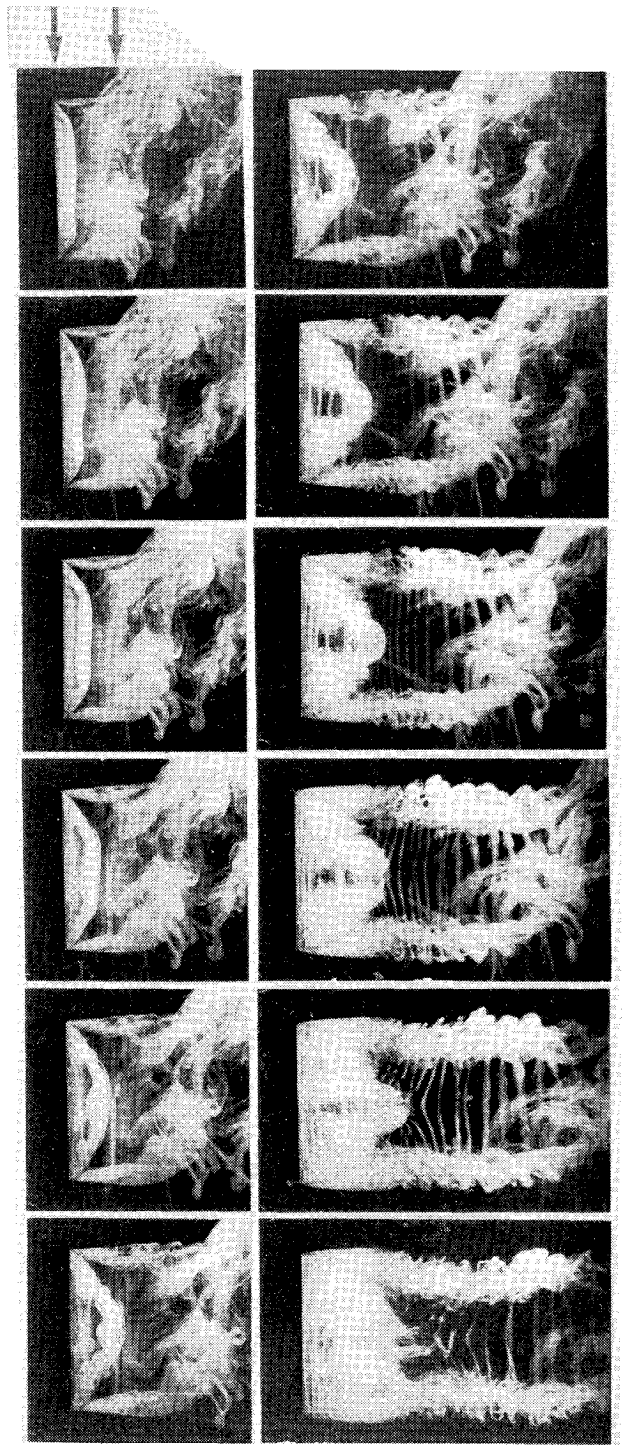

Fig. 4 Visualization sequence for rectangular wing with an aspect ratio 2.

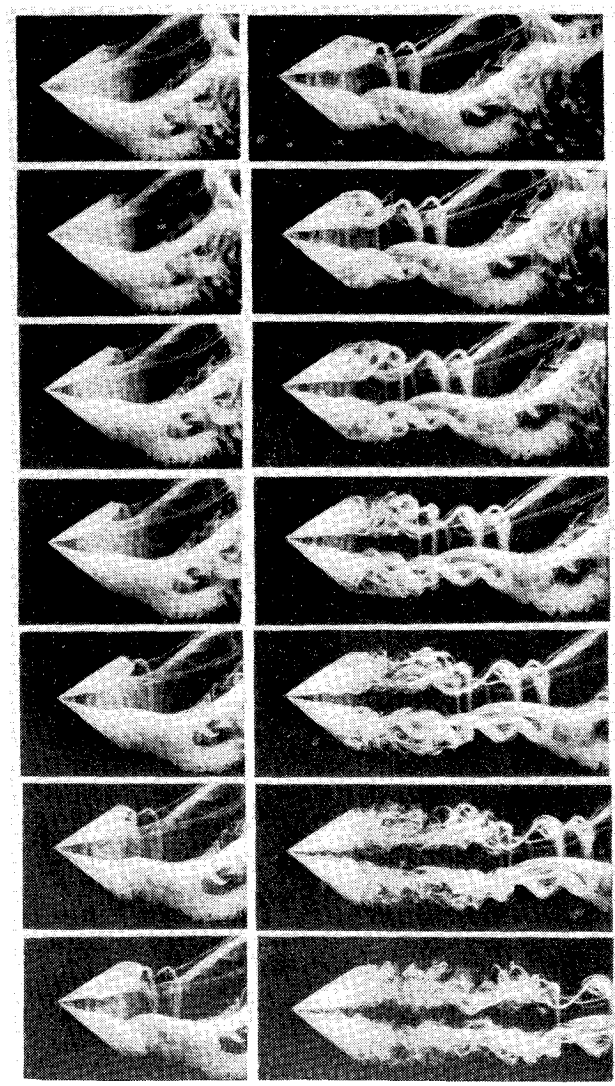

Fig. 5 Visualization sequence for a delta wing.

istic time scale is $t_c = 0.25$ s and the Reynolds number $R = 5200$ according to Eqs. (1) and (3), respectively.

Experimental Results

Wing Shapes and Other Data

In this section, we present photographic sequences for rectangular, delta, sail, and circular wings. Figure 2 shows the planforms, dimensions, and the figure numbers of the visualization sequences for these wings. Each sequence is presented as a figure composed of frames. Frames of a sequence are ordered into columns from top to bottom and then across columns from left to right. Consecutive frames are always the same time $\Delta t = 1/16$ s apart from each other, corresponding to a dimensionless time difference $\Delta t^* = \Delta t/t_c = 0.25$. The time from flow startup to the first frame shown was always $t_1 = 12/64$ s or $t_1^* = t_1/t_c = 0.75$. Flow is always from left to right. As already mentioned, the angle of attack for each figure is $\alpha = 40$ deg and the Reynolds number is $R = 5200$. Since these data were the same for all figures, they will not be listed in the figure captions.

Rectangular Wings

Figure 3 represents a visualization sequence for a square wing (15.2×15.2 cm). For easy orientation, the leading and trailing edges of the wing have been marked by arrows on top of the first frame.

The first column of the figure shows, among other flow developments, the formation of an arching leading-edge vortex structure anchored to the front corners of the wing. In the lower frames of the first column, the arch forms an Ω-shaped vortex that turns into a turbulent vortex ring or puff in column 2. Turbulent dissipation is so strong that in the lower frames of column 2 the puff can no longer be identified. Meanwhile, a vortex sheet leaves the trailing edge and, because of the Kelvin-Helmholtz instability, forms vortices visible as vertical smoke bands in the lower frames of column 1 and more clearly in column 2. These vortices turn toward the wing tips where they interweave with each other to form conical tip vortices. The apex of the upper tip vortex is located at the upper front corner of the wing and the apex of the lower tip vortex is located at its lower front corner. At these corners, the tip vortices join with the leading-edge vortex structure to form, in essence, a system of closed vortices. Such a view is in accordance with Helmholtz's law, which for a viscous flow over a nonrotating body states that a finite system of vortices must be closed. That trailing-edge vortices form by Kelvin-Helmholtz instability has become clear from the abundant number of examples of two-dimensional cuts that have been shown by Freymuth[13] for starting flow over airfoils.

A rather similar development occurred also in the case of a larger aspect ratio. Figure 4 shows visualization for a wing with a span twice as long (30.4 cm) than the chord. The last few frames show an interaction between the leading- and trailing-edge vortex structure near the wake centerline and prior to blurring by the turbulence.

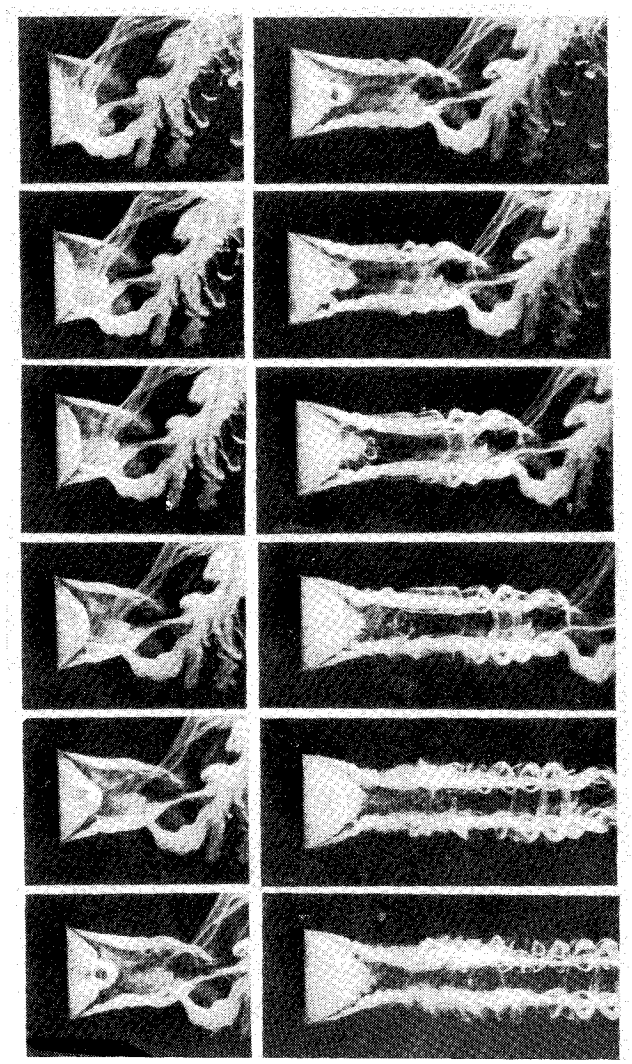

Fig. 6 Visualization sequence for a delta wing in reverse.

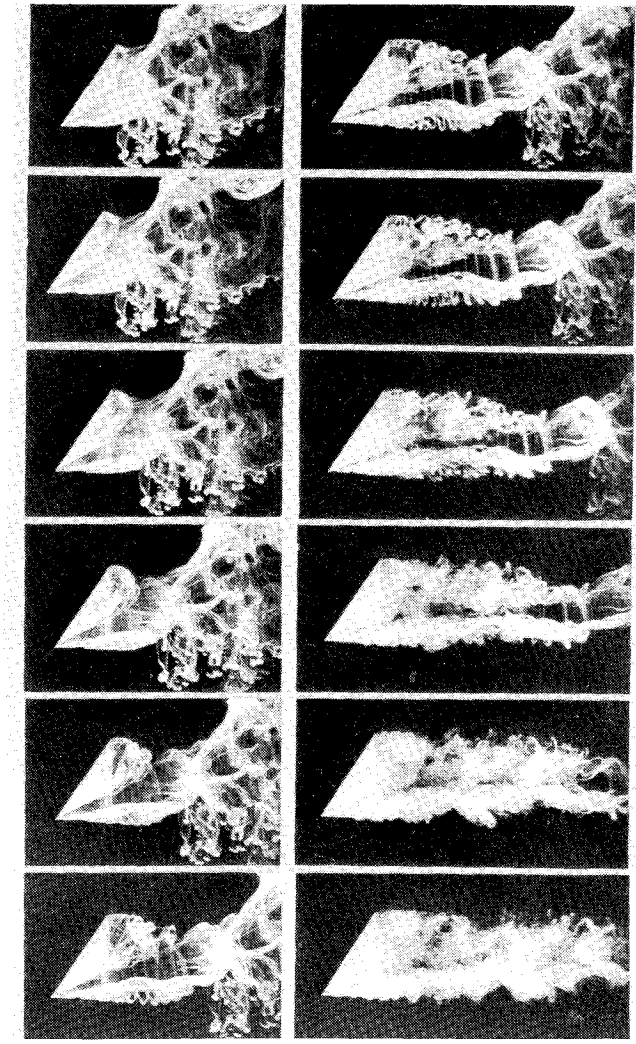

Fig. 7 Visualization sequence for a sail wing.

It has to be mentioned that, in addition to the developing vortex system, remnants of smoke introduction from the time prior to flow startup and other inhomogeneities in the smoke introduction somewhat degrade the visualization. A decrease of this "optical noise" is a difficult goal of future development efforts.

Delta Wings

Figure 5 visualizes the development of the starting vortex system of a flat delta wing. Its planform and dimensions have been shown in Fig. 2 and the angle of attack is again $\alpha = 40$ deg.

The left column shows the development of conical tip vortices near the leading edges of the delta wing. The apex of each of the two cones is located at the front corner where the cones thus join. Furthermore, the development near the upper leading edge reveals an arching of the tip vortex toward the upper trailing-edge corner. Simultaneously, a vortex sheet leaves the trailing edge and starts to form several trailing-edge starting vortices due to the Kelvin-Helmholtz instability. Column 2 shows more clearly these trailing-edge starting vortices, which bend upstream and connect to the leading-edge tip vortices. Therefore, the trailing-edge starting vortices represent a system of intertwined vortex loops feeding into the conical tip vortices and forming a closed vortex system in accordance with Helmholtz's law. The trailing-edge vortex system is, therefore, similar to the corresponding trailing-edge system of intertwined vortex loops of Figs. 3 and 4 for rectangular wings. In the upper frames of column 2, the leading-edge tip vortices assume a multihelical structure. The onset of turbulence blurs details in the lower frames of column 2.

Figure 6 visualizes the starting vortex system for the delta wing mounted in reverse. In this case, a side of the equilateral triangle heads into the flow rather than a corner. The leading-edge starting vortex develops similar to the one for the square wing (Fig. 3) in column 1, i.e., an Ω vortex develops and dissipates turbulently in column 2. Also, the combined system of trailing starting vortices and tip vortices forming intertwined vortex loops, anchored to the front corner of the wing, resemble those for the square wing except that they form a narrower wake.

Sail Wings

Figure 7 displays the vortex development over a triangle with two 45 deg angles. The planform of this triangle is shown in Fig. 2, in which it is labeled a sail wing. Angle of attack again is $\alpha = 40$ deg. Due to the asymmetry of the configuration, the developing closed vortex system is also asymmetric in appearance. The leading-edge starting vortex forms an asymmetric arch anchored to the front and top corners of the wing in column 1. Near the upper corner, a series of intertwined but very small vortex loops seems to form in the upper frames of column 2, giving them the appearance of a lace pattern. This detail is, however, quickly blurred by tur-

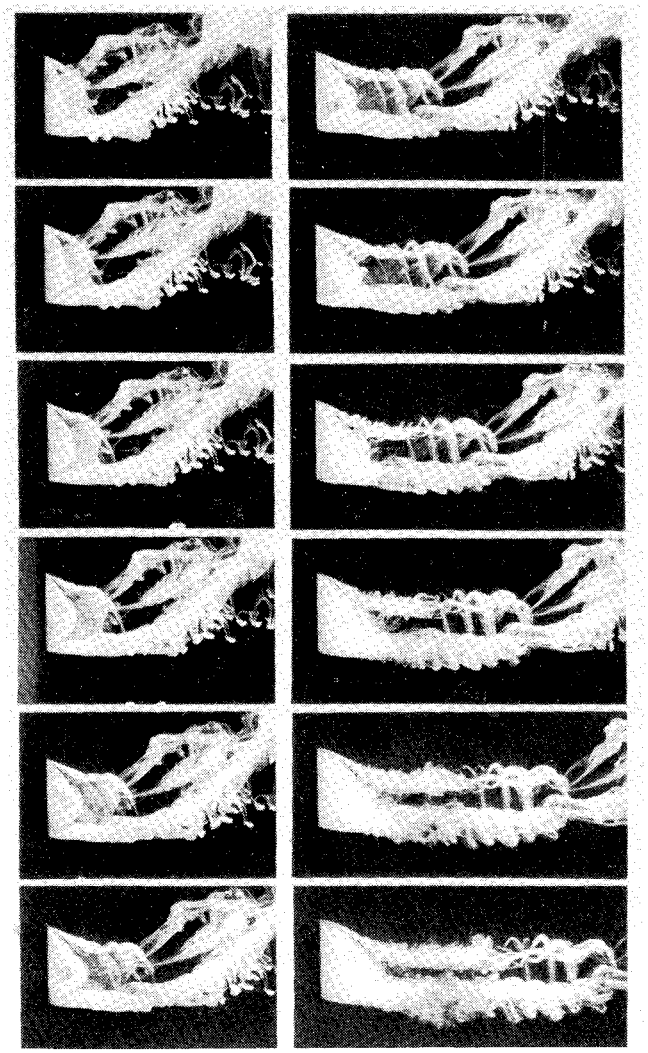

Fig. 8 Visualization sequence for a sail wing in reverse.

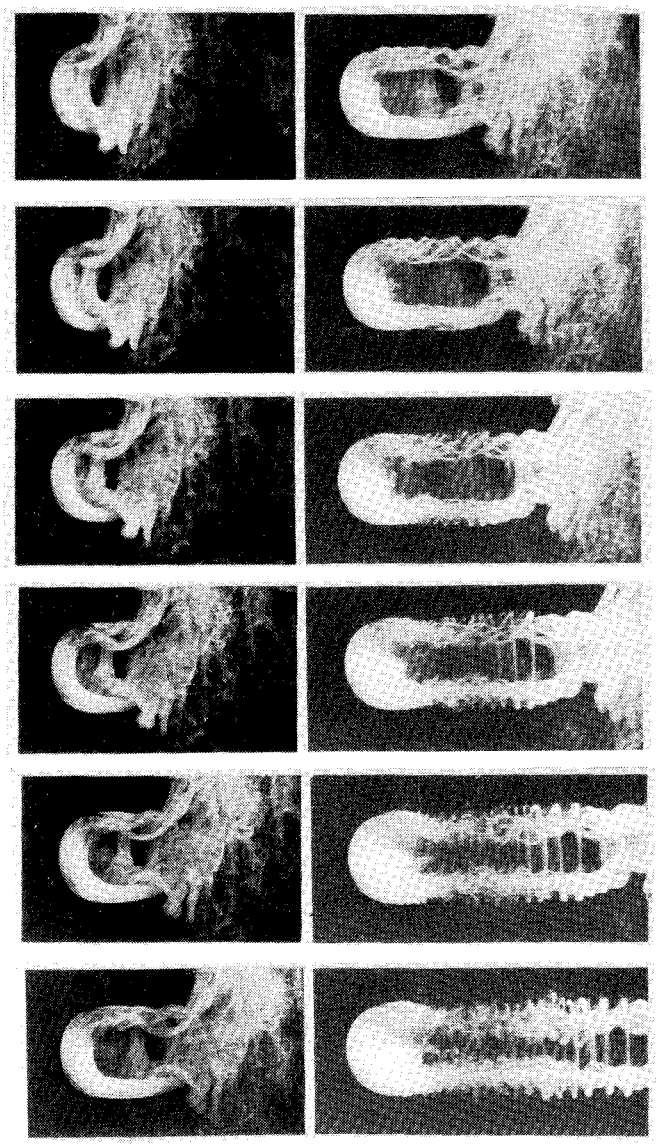

Fig. 9 Visualization sequence for a circular wing.

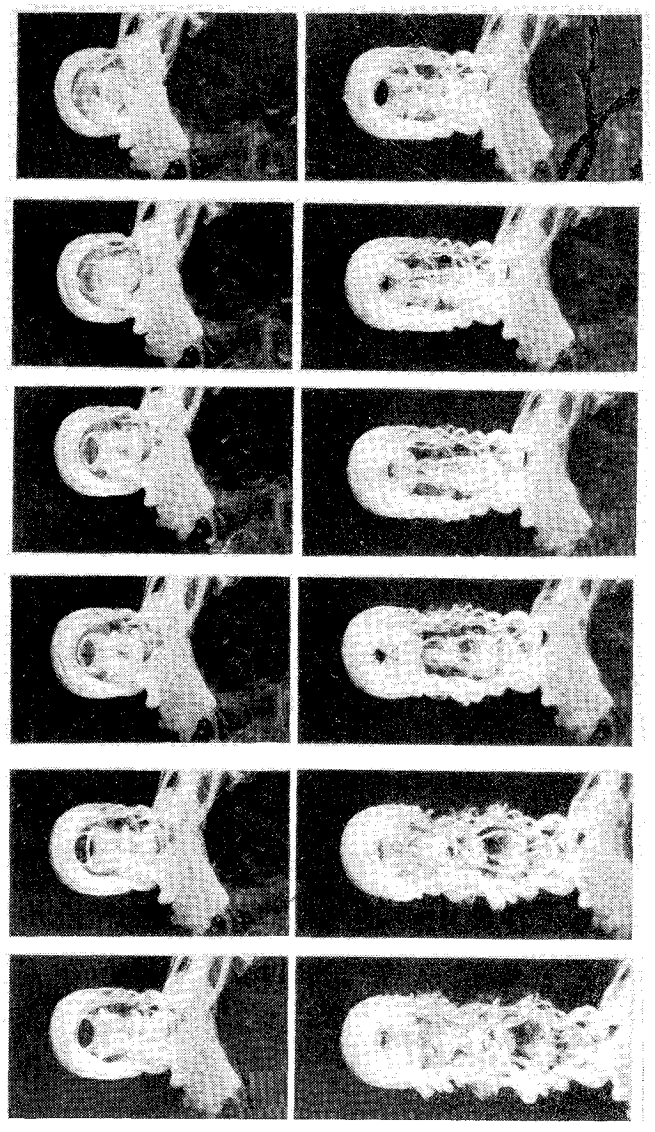

Fig. 10 Visualization sequence for a circular wing with a center hole.

bulence. The trailing-edge system of much larger intertwined vortex loops connects to the bottom tip and leading-edge vortices of multihelical and conical shape. On the top, the leading-edge vortex seems to loose its upper anchor at the top corner in the lower frames of column 1 and the upper frames of column 2. Any detail is blurred by turbulence in the lower frames of column 2.

The sail wing in reverse where a side of the triangle heads into the wind, is visualized in Fig. 8. Column 1 shows the familiar leading-edge arching vortex from which a slightly asymmetric Ω vortex develops. The trailing-edge system of vortex loops anchored to the top and bottom front corners of the wing in the form of conical tip vortices are fully visualized in column 2. The trailing-edge wake narrows down from the top, but roughly follows the tunnel flow near the bottom edge of the wake.

Circular Wings

Figure 9 visualizes the starting vortex system for a circular flat plate at a 40 deg angle of attack. Again, a closed system of vortex filaments develops, resembling the shape of a rubber raft in the upper frames of column 2 and prior to onset of turbulence.

Figure 10 visualizes the starting vortex system of a circular wing with a round hole at its center. The vortex system generated by the outer contour of the wing resembles that of Fig. 9, while the center hole produces vortex rings that subsequently interact with the outer wake to increase the level of turbulence.

Conclusions

The combined wing tip and starting vortex systems of a variety of wing planforms have been visualized in accelerated starting flow at an angle of attack $\alpha = 40$ deg and at a Reynolds number $R = 5200$. Visualizations at other angles of attack and other Reynolds numbers have also been done, but are not included here since nothing qualitatively new has been found. Basic vortex elements identified by us are intertwined vortex loops usually anchored to wing corners in the form of multihelix conical tip vortices. In addition, the visualizations reveal the development of Ω and ring vortices. In the late stages of development, the turbulence blurs much of the detail.

Our visualizations should go a long way to fill in some of the details of the concept of a combined wing tip and starting vortex system that was advanced 70 years ago. Further investigation of other unsteady configurations, such as impulsively started wings and steady flow over pitching wings, should clarify the concept even further.

Acknowledgment

This work has been supported by the U. S. Air Force Office of Scientific Research, Contract F49620-84-C-0065, Dr. J. McMichael, project manager.

References

[1]Prandtl, L., "Tragflächen-Auftrieb und Widerstand in der Theorie," *Jahrbuecher der Wissenschaftliche Gesellschaft für Luftfahrt*, Vol. 5, 1920, pp. 37–55.

[2]Prandtl, L., "The Generation of Vortices in Fluids of Small Viscosity," *Journal of the Royal Aeronautical Society*, Vol. 31, May 1927, pp. 720–743.

[3]Kutta, W. M., "Auftriebskräfte in Strömenden Flüssigkeiten," *Illustr. Aeron. Mitt.*, Vol. 6, 1902, pp. 133–135.

[4]Tani, I., "The Wing Section Theory of Kutta and Zhukovski," *Recent Developments in Theoretical and Experimental Fluid Mechanics*, Springer-Verlag, New York, 1979, pp. 512–516.

[5]Lanchester, F. W., *Aerodynamics*, Constable & Co., Ltd., London, 1907.

[6]von Kármán, T., *Aerodynamics*, Cornell University Press, Ithaca, NY, 1954.

[7]Rogers, E. W. E., "Aerodynamics—Retrospect and Prospect," *Aeronautical Journal of the Royal Aeronautical Society*, Feb. 1982.

[8]Gad-el-Hak, M. and Ho, C. M., "Unsteady Vortical Flow Around Three-Dimensional Lifting Surfaces," *AIAA Journal*, Vol. 24, May 1986, pp. 713–721.

[9]Gad-el-Hak, M. and Ho, C. M., "The Pitching Delta Wing," *AIAA Journal*, Vol. 23, Nov. 1985, pp. 1660–1665.

[10]Adler, J. N. and Luttges, M. W., "Three Dimensionality in Unsteady Flow About a Wing," AIAA Paper 85-0132, 1985.

[11]Werlé, H., "Visualization Hydrodynamique D'Écoulements Instationnaires," ONERA Note Technique 180, 1971.

[12]Werlé, H., "Structures des Décollements Sur les Ailes Cylindriques," Recherche Aerospatiale 1986-3, May–June 1986, pp. 221–242.

[13]Freymuth, P., "The Vortex Patterns of Dynamic Separation: A Parametric and Comparative Study," *Progress in Aerospace Sciences*, Vol. 22, 1985, pp. 161–208.

[14]Freymuth, P., "Visualizing the Combined System of Wing Tip and Starting Vortices," *TSI Flowlines*, Vol. 1, May 1986.

[15]Freymuth, P., Finaish, F., and Bank, W., "The Wing Tip Vortex System in a Starting Flow," *Zeitschrift für Flugwissenschaften und Weltraumforsch*, Vol. 10, March-April 1986, pp. 116-118.

[16]Freymuth, P., Finaish, F., and Bank, W., "Visualization of Wing Tip Vortices in Accelerating and Steady Flow," *Journal of Aircraft*, Vol. 23, Sept. 1986, pp. 730-733.

[17]Lugt, H. J. and Haussling, H. J., "Laminar Flow Past an Abruptly Accelerated Elliptic Cylinder at 45° Incidence," *Journal of Fluid Mechanics*, Vol. 65, Dec. 1974, pp. 711-734.

[18]Leben, R. R., "Multigrid Calculation of Boundary-Fitted Orthogonal Coordinates With Applications to Unsteady Flows," Ph.D Thesis, Dept. of Aerospace Engineering Sciences, University of Colorado, Boulder, 1986.

[19]Sheen, Q., "Potential Flow Analysis of Unsteady Joukowsky Aerofoil in the Presence of Discrete Vortices," Ph.D. Thesis, Dept. of Aerospace Engineering Sciences, University of Colorado, Boulder, 1986.

[20]McCroskey, W. J., "Unsteady Airfoils," *Annual Review of Fluid Mechanics*, Vol. 14, 1982, pp. 285-311.